J. Biochem. 121, 654-660 (1997)

Remarkable Functional Aspects of Myoglobin Induced by Diazaheme Prosthetic Group[1]

Saburo Neya,*,[2] Hiroshi Hori,† Kiyohiro Imai,‡ Yasuko Kawamura-Konishi,§ Haruo Suzuki,§ Yoshitsugu Shiro,‖ Tetsutaro Iizuka,‖ and Noriaki Funasaki*

**Department of Physical Chemistry, Kyoto Pharmaceutical University, Yamashina-ku, Kyoto 607; †Department of Biophysical Engineering, Faculty of Engineering Science, Osaka University, Toyonaka, Osaka 560; ‡Department of Physicochemical Physiology, Medical School, Osaka University, Suita, Osaka 565; §Department of Biosciences, School of Science, Kitasato University, Sagamihara, Kanagawa 228; and ‖Institute of Physical and Chemical Research (RIKEN), Saitama 351-01*

Received for publication, October 15, 1996

The iron complex of β,δ-diazamesoporphyrin III, a molecular hybrid of porphyrin and phthalocyanine, was incorporated into apomyoglobin to investigate novel biological aspects of myoglobin. The reconstituted ferric protein forms an internal hemichrome with the iron-bound distal histidine. The reduced ferrous protein has extraordinarily high affinities for O_2 and CO. The ferrous myoglobin is capable of strong binding with pyridine, imidazole, cyanide, and azide, and reacts moderately with ammonia. The NO complex exhibited 5-coordinate to 6-coordinate transition over 150 min. The instability of 5-coordinate NO heme is consistent with a high affinity of imidazole to the ferrous heme. The kinetic analyses of the ferrous derivatives suggest the importance of the π orbitals in neutral ligands as well as the negative charges in anionic ligands. A high affinity of imidazole to ferrous diazaheme accounts for the internal hemochrome formation in ferrous myoglobin containing phthalocyanines.

Key words: coordination structure, β,δ-diazamesoporphyrin, electronic spectra, ligand binding, myoglobin.

Modified hemes have been used to perturb the biological and spectroscopic properties of hemoproteins. Replacement of the meso carbons of heme with nitrogen atoms affords azaporphyrins, of which the familiar is the tetraaza compound, phthalocyanine (*1*). Several reports on the phthalocyanine-bound myoglobin (Mb) have been appeared (*2-4*). Diazaporphyrin, a molecular hybrid of porphyrin and phthalocyanine, contains two nitrogen atoms linking the two pyrromethene units (*5-7*). The diazaporphyrin bearing two propionate groups has not been characterized as a prosthetic group of hemoprotein. We have prepared a diaza macrocycle, β,δ-diazamesoheme III (inset, Fig. 1), in an attempt to introduce diazaheme into the protein matrix and to examine its influence on the biological function. The reconstituted Mb, Mb(diazaheme), bridges a large interstice between the phthalocyanine-substituted Mb and native Mb. Detailed examination of Mb(diazaheme) might reveal novel biological aspects of Mb. Substantially intriguing spectroscopic signatures and biological properties are expected for the Mb while little is known about it. We report herein the first analyses on Mb(diazaheme).

[1] This work was supported by grants from the Scientific Research Foundation of Kyoto Pharmaceutical University, the Ministry of Education, Science, Sports and Culture of Japan (#07308071), and the Japan Private School Promotion Foundation.

[2] To whom correspondence should be addressed. Tel: +81-75-595-4664, Fax: +81-75-595-4762

Abbreviations: EPR, electron paramagnetic resonance; Mb, myoglobin; Tris, tris(hydroxymethyl)aminomethane.

MATERIALS AND METHODS

β,δ-Diazamesoporphyrin III and Iron Porphyrin—The title porphyrin was synthesized through the coupling of two kinds of dibromopyrromethenes. The free bases of 5,5′-dibromo-3,3′-diethyl-4,4′-dimethyldipyrromethene (*8*) (2.00 g, 5.18 mmol) and 5,5′-dibromo-3,3′-di(methoxycarbonylethyl)-4,4′-dimethyldipyrromethene (*9*) (2.60 g, 5.18 mmol), and sodium azide (10 g, 154 mmol) were placed in a round-bottomed flask containing 1,000 ml of methanol, and the mixture was gently refluxed for 72 h. After solvent evaporation, the residue was chromatographed (silica gel, chloroform). Three diazaporphyrins, as expected from the coupling of the two pyrromethenes, were found. The most and least mobile bands were identified as β,δ-diazaetioporphyrin II and β,δ-diazacoproporphyrin II (*6*), respectively, based on the proton nuclear magnetic resonance spectra (Varian XL-300, 300 MHz). β,δ-Diazamesoporphyrin III was eluted as the intermediate fraction. The solution was concentrated, mixed with an equal volume of methanol, and slowly evaporated under low heating to afford β,δ-diazamesoporphyrin III as deep-purple fluffy microneedles (238 mg, 7.7%). $C_{34}H_{40}N_6O_4$ requires C, 68.37; H, 6.70; N, 14.08: Found C, 68.19; H, 6.46; N, 14.07. *m/e* 595 (M+) for 595.7. δ_H −3.17 (2H, br, NH), 1.82 (6H, t, CH_2CH_3), 3.24 (4H, t, CH_2CH_2CO), 3.57 and 3.60 (each 6H, s, ring CH_3), 3.63 (6H, s, OCH_3), 3.98 (4H, q, CH_2CH_3), 4.32 (4H, t, CH_2CH_2CO), 9.93 (1H, s, meso H), and 10.00 (1H, s, meso H). λ_{max} (ε) in chloroform; 373 nm (104 mM^{-1}·

cm^{-1}), 515 (shoulder, 8.5), 545 (29.6), 567 (8.5), and 620 (49.5).

The iron complex of the dimethylester was prepared by reaction with ferrous chloride in refluxing dimethylformamide (*10*). The resultant hemin chloride, obtained *via* air oxidation, was purified on a silica gel column with chloroform-methanol (9 : 1, v/v). Values of λ_{max} (ϵ) in chloroform; 349 nm (91.0 $mM^{-1}\cdot cm^{-1}$), 471 (16.0), 572 (17.8), 632 (5.3), and 690 (6.5). The hemin dimethylester was hydrolyzed (*11*), precipitated with hydrochloric acid, and then dried. The spectrum of the pyridine hemochromogen, prepared after reduction with sodium dithionite, was characterized in a 0.1 M NaOH-pyridine (1 : 1, v/v) mixture; 395 nm (66.7 $mM^{-1}\cdot cm^{-1}$) and 577 (87.0).

Reconstituted Mb—Sperm whale Mb was purchased from Sigma (type II). Mb(diazaheme), a Mb substituted with β,δ-diazamesohemin III, was prepared and purified by means of the procedures reported for Mb(monoazaheme) (*12*). The reconstitution proceeded smoothly and the yield was better than 80%. Purified ferric Mb(diazaheme) was determined at 375 nm (86 $mM^{-1}\cdot cm^{-1}$).

Spectroscopy and Physical Measurements—Visible absorption spectra were recorded with a Shimadzu MPS-2000 spectrophotometer equipped with a thermostated cell compartment. EPR spectra were obtained at X-band (9.35 GHz) microwave frequency by using a Varian cavity with a Varian E-12 EPR spectrometer with 100 kHz field modulation (0.5 mTesla). An Oxford flow cryostat (ESR-900) was used for liquid-helium temperature measurements. Ligand binding constants were estimated by optical titration. Oxygen equilibrium curves were recorded on an automatic recording apparatus (*13*) in the presence of an enzymic reducing system (*14*). The association of pyridine and imidazole with deoxy Mb was monitored with an Applied Photophysics stopped-flow apparatus, SX-17MV, with a thermostated sample holder. The photolysis of the O_2 and CO Mbs was attempted with a flash-photolysis apparatus (UNISOK, Osaka) by using a 250 mJ extinction flash of 250 ns at 591 nm. The slow binding of cyanide or azide to the deoxy Mb was measured with a Shimadzu MPS-2000 spectrophotometer. The CO affinity was estimated by titrating CO-saturated 0.1 M Tris buffer against ferrous pyridine complex of the Mb at 20°C, where the CO concentration in water was assumed to be 1,014 μM (*15*).

RESULTS

Acidity of the Free Base—The acid-base properties of the free base diazaporphyrin are expected to be seriously perturbed by the two electronegative meso-nitrogen atoms. We quantitatively estimated the acidity of β,δ-diazamesoporphyrin III in aqueous 2.5% sodium dodecylsulfate. No appreciable spectral changes occurred between pH 6 and 4. However, with further decrease of the pH to 0.4, remarkable visible peak shifts from 618 to 640 nm took place with a well-defined isosbestic point at 630 nm. Although the

TABLE I. **Visible absorption parameters of the Mb containing β,δ-diazamesohemin III.**

Ligand	$\lambda(\epsilon)$[a]			
Ferric				
None[b]	374 (86.0)	567 (22.1)	678 (4.0)	
CN^-	376 (71.1)	565 (27.3)		
N_3^-	376 (72.3)	557 (25.4)		
Pyridine	378 (78.1)	565 (29.7)		
Imidazole	376 (82.4)	540_{sh}[c]	554 (29.5)	
NH_3	378 (74.7)	569 (28.1)		
Ferrous				
Deoxy	380_{sh} (~65)	546 (21.3)	583 (19.6)	660 (3.0)
O_2	380 (56.1)	580 (24.9)		
CO	383 (66.3)	571 (44.8)		
	403 (65.1)			
CN^-	380 (80.6)	538 (10.7)	620 (19.1)	663 (42.4)
N_3^-	400_{sh} (~55)	582 (38.2)		
Pyridine	395 (69.3)	526 (19.7)	558 (32.0)	577 (86.0)
Imidazole	400 (66.3)	529 (17.1)	563 (27.5)	583 (67.5)
NH_3[d]	399 (52.3)	529 (14.9)	563 (24.2)	582 (56.1)

[a]Wavelength in nm (and extinction coefficient in $mM^{-1}\cdot cm^{-1}$) measured in 0.1 M Tris at pH 7.0 and 20°C. Ferrous derivatives were obtained after reduction with $Na_2S_2O_4$. [b]Ferric Mb(diazaheme) is a hemichrome with iron-bound distal histidine. [c]$_{sh}$, shoulder peak. [d]Measured in 0.05 M borate at pH 9.0 and 20°C.

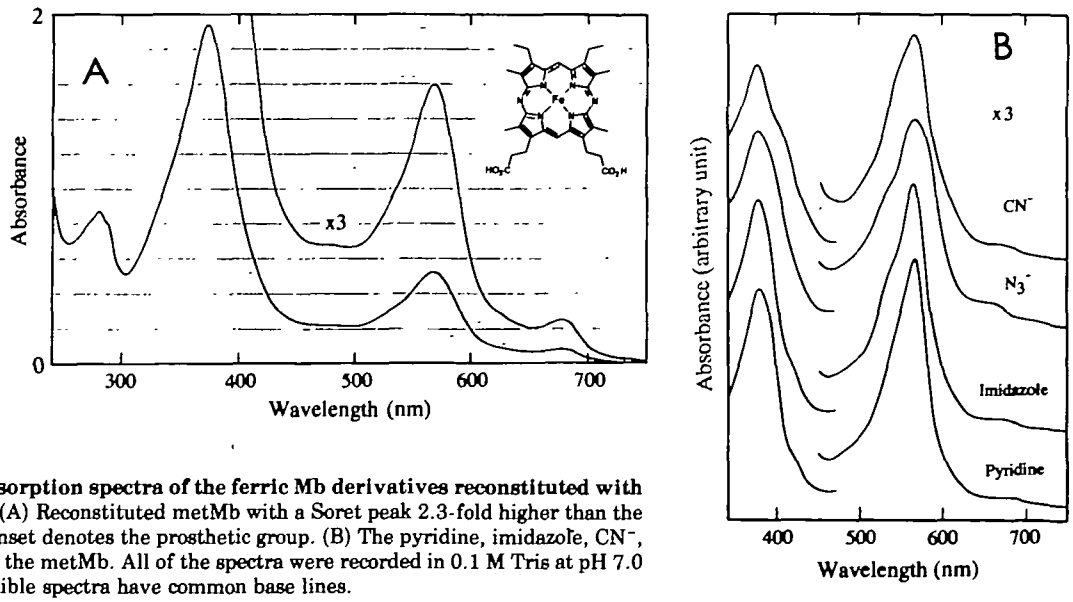

Fig. 1. **The electronic absorption spectra of the ferric Mb derivatives reconstituted with β,δ-diazamesohemin III.** (A) Reconstituted metMb with a Soret peak 2.3-fold higher than the 280-nm protein band. The inset denotes the prosthetic group. (B) The pyridine, imidazole, CN^-, N_3^-, and NH_3 derivatives of the metMb. All of the spectra were recorded in 0.1 M Tris at pH 7.0 and 20°C. The Soret and visible spectra have common base lines.

optical transitions could not be followed completely, the 640-nm absorbances can be appropriately simulated with the Henderson-Hasselbalch equation, yielding an apparent pK of 0.66±0.05 (results not shown). The transition was assigned to the third protonation at the pyrrole nitrogen (pK_3) rather than at the meso nitrogen, because the latter is known to be protonated only in concentrated sulfuric acid (*5, 16*). The pK_3 value of diazaporphyrin is 5 pH unit lower than that (5.8) of a reference compound, mesoporphyrin (*17*).

Ferric Mb—The optical titration of the apoMb with the ferric diazamesohemin, as monitored at 390 nm, revealed a 1:1 complex formation. Figure 1 shows the electronic absorption spectrum of the purified ferric Mb. The 374-nm Soret peak is higher by 2.3-fold than the 280-nm protein band even after intensive purification. As the prominent 567 nm peak indicates, ferric Mb(diazaheme) is violet. The ferric Mb(diazaheme) does not show any spectral transition between pH 7 and 10. Cyanide, azide, imidazole, pyridine, and NH_3 coordinate to the ferric heme with affinities (in M^{-1}) of 8.6×10^4, 6.8×10^4, 4.0×10^3, 130, and 5.2, respectively, all measured in 0.1 M Tris at pH 7.0 and 20°C. These values are approximately two orders of magnitude lower than those reported for native Mb (*18*). Fluoride induced no appreciable spectral change even at 5 M and presumably failed to bind. The visible spectra of the ferric derivatives are summarized in Fig. 1 and Table I. We recorded the EPR spectra to examine further the coordination state of the Mb. The EPR in Fig. 2 with $g=2.79$, 2.28, and 1.76, recorded in the absence of exogenous ligand, is typical of a low-spin compound. In contrast, the g values for the cyanide and azide derivatives are similar to those of the native Mb derivatives (*19*).

Ferrous Mb—In remarkable contrast to native Mb, cyanide, azide,[3] pyridine, and imidazole bind to ferrous Mb(diazaheme). In the part A of Fig. 3, the optical titration of cyanide against the deoxy protein, which is accompanied with remarkable color changes from violet to bright green, is illustrated. The affinity of cyanide was 8,300 M^{-1} at pH 7.0. Part B of Fig. 3 presents a kinetic trace for azide binding. From the optical traces, the k_{on} and k_{off} rate constants for azide were estimated to be 7.3×10^{-2} $M^{-1}\cdot s^{-1}$ and $8.2\times10^{-4}\cdot s^{-1}$, respectively. Pyridine (1.1×10^4 M^{-1}) and imidazole (200 M^{-1}) have high equilibrium affinities for ferrous Mb(diazaheme). Association rates of pyridine and imidazole to deoxy Mb(diazaheme) were monitored with a stopped-flow apparatus, the results being compiled in Table II. A nonaromatic Lewis base, NH_3, also binds to

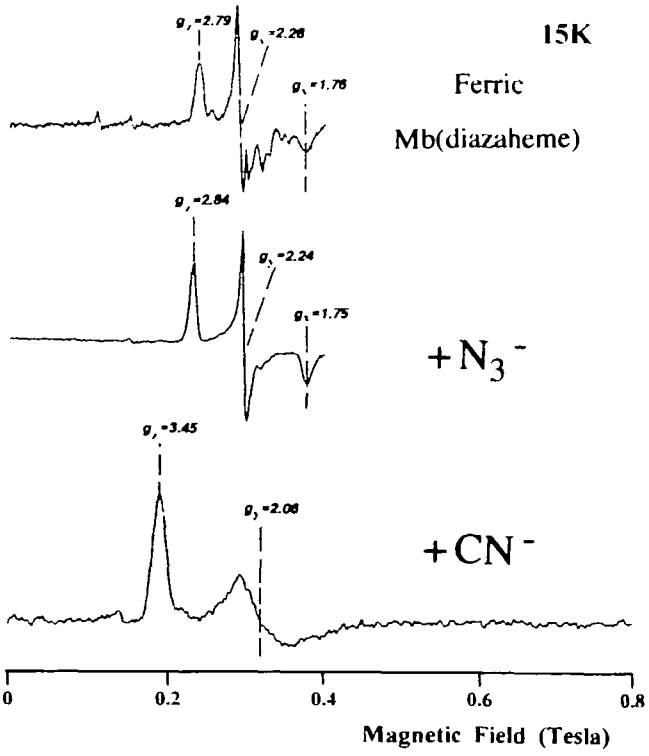

Fig. 2. **EPR spectra of the ferric Mb(diazahemin) derivatives at 15 K.** The heme concentration is 2 mM in 0.1 M Tris at pH 7.0.

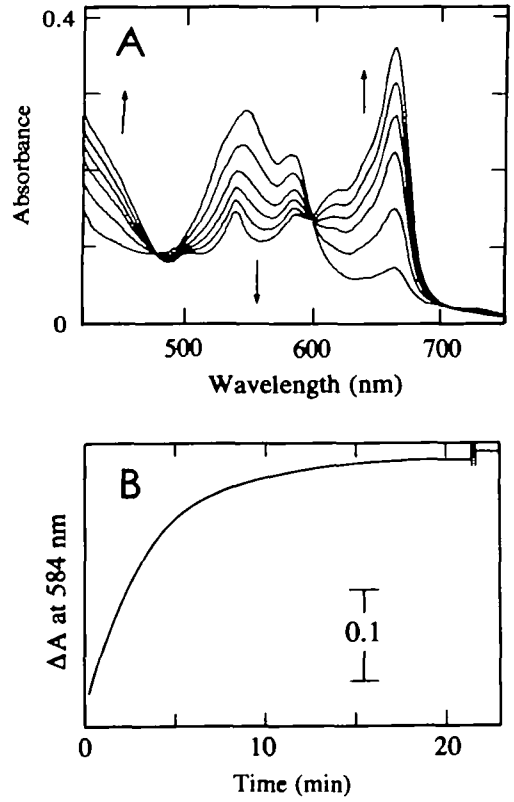

Fig. 3. **Ligand binding to deoxy Mb(diazaheme).** (A) Equilibrium CN^- binding. CN^- concentration was increased from 0 to 22.9, 45.9, 74.5, 120, and 177 μM in 0.1 M Tris at pH 7.0 and 20°C, as indicated by the arrows. (B) Kinetic trace of N_3^- binding in 0.1 M Tris at pH 7.0 and 20°C in the presence of 12 μM Mb and 50 mM NaN_3.

[3] We have erroneously reported that azide does not bind to deoxy Mb(monoazaheme) (*12*). This arose because of the visible spectral similarity between the ferric and ferrous azide derivatives and a weak binding of azide to the ferrous Mb. We reexamined spectrophotometric titration of NaN_3 and confirmed the formation of ferrous Mb(monoazaheme)N_3^- with 1.9 M^{-1} in 0.1 M Tris at pH 7.0 and 20°C. The ferrous azide complex was also produced by reducing ferric Mb(monoazaheme)N_3^- with sodium dithionite. The reduction proceeded over 40 min with well-defined isosbestic points at 362, 400, 559, and 683 nm. The visible spectrum of ferrous Mb(monoazaheme)-N_3^-, 396 nm (82.0 $mM^{-1}\cdot cm^{-1}$), 535 (9.8), and 566 (23.2), was characterized in 0.1 M Tris containing 3 M NaN_3 at pH 7.0 and 20°C.

TABLE II. **Kinetic parameters (accurate to ±20%) for the deoxy Mb reconstituted β,δ-diazamesoheme III in 0.1 M Tris at pH 7.0 and 20°C.**

Ligand	k_{on} ($M^{-1}\cdot s^{-1}$)	k_{off}[a] (s^{-1})	K (M^{-1})
CN^-	8.0×10^{-2}	9.7×10^{-6}	8,300
N_3^-	7.3×10^{-2}	8.2×10^{-4}	89
Pyridine	9.6×10^{4}	8.7	11,000
Imidazole	3.4×10^{3}	17	200

[a]Dissociation rate was calculated as k_{on}/K.

the ferrous Mb. Titration of aqueous NH_3 in 0.05 M borate at pH 9.0 and resulted in visible spectral transitions with an isosbestic point at 559 nm (1.7 M^{-1}), although NH_4Cl at pH 7.0 did not cause spectral changes. Figure 4 and Table I summarize the visible spectra of various Mb(diazaheme) derivatives. The strong visible bands of the ferrous pyridine and imidazole derivatives are notable.

O_2, CO, and NO Bindings—The reduced Mb(diazaheme) is capable of binding the conventional gaseous ligands. The Soret band of Mb(diazaheme)CO is lowered while the visible peaks are intensified (part A, Fig. 5), as compared with native Mb. Of equal interest, the Soret band of Mb(diazaheme)CO is clearly split into two bands. The visible spectra of the CO, O_2, and deoxy derivatives are summarized in Table I. The Hill plots of the O_2 binding (part B, Fig. 5) afforded values of $n=1.15$ and $P_{50}=0.018$ mmHg. The CO affinity was estimated by CO titration of the ferrous pyridine complex. The partition coefficient [Mb·CO][pyridine]/[Mb·pyridine][CO] was calculated to be 7.7×10^4 (part C, Fig. 5). From the pyridine binding constant to the deoxy Mb, we obtained an affinity of 8.5×10^6 M^{-1} for CO. The ligation of NO was monitored with EPR (Fig. 6). The freshly prepared NO Mb(diazaheme) is 5-coordinate as evidenced by the characteristic three-line hyperfine pattern. The 5-coordinate MbNO gradually turned into a 6-coordinate structure, and only the 6-coordinate species remained after 2.5 h incubation in an ice bath. This is in remarkable contrast with native MbNO which remains 6-coordinate. The attempted kinetic measurements for the O_2, CO, and NO derivatives by flash photolysis were unsuccessful because they were apparently not photodissociable, probably because of either low quantum yields or extremely rapid reaction beyond the time resolution limit.

DISCUSSION

Myoglobin with Diazaheme—The stoichiometry of heme binding and functional integrity suggest the incorporation of the diazahemin into the heme pocket. The absence of the acid-alkaline transition provides evidence that the distal histidine binds to the ferric heme to form a hemichrome. Ligation of the distal histidine is not anomalous, because it also occurs upon insertion of an unnatural synthetic heme (*20*). The hemichrome structure in our sample is supported by the low-spin EPR signals. The less anisotropic g values (2.79, 2.28, and 1.76), as compared with those ($g=2.91$, 2.26, and 1.53) of native metMb complexed with imidazole (*19*), suggest an anomalous coordination of the distal imidazole or a strained iron-distal imidazole bond. Since the EPR parameters in the azide and cyanide derivatives are closely similar between ferric Mb(diazahemin) (Fig. 2) and native Mb (*19*), the different g values are unlikely to reflect the heme variation. Rather, there may be lower electronic symmetry in the diazaheme than in the imidazole complex of native Mb (*19*). Hemichrome formation in the ferric Mb is consistent with the ligand affinities being two orders of magnitude lower than those found for native Mb.

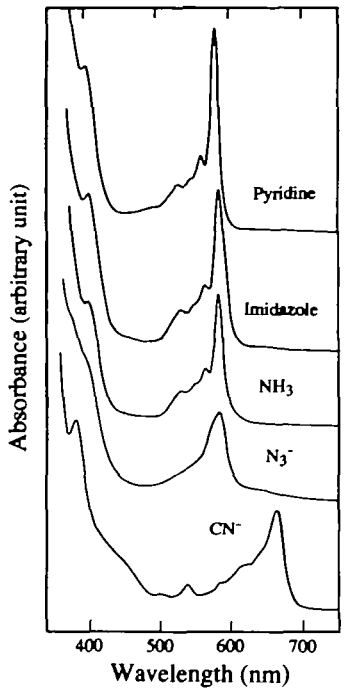

Fig. 4. **Visible spectra of the ferrous Mb(diazaheme) derivatives.** Recorded in 0.1 M Tris at pH 7.0 and 20°C, except for the NH_3 complex (recorded in 0.05 M borate at pH 9.0 and 20°C).

The spectral comparison of Mb(diazaheme)CO in Fig. 5 with native MbCO [$\varepsilon_{423}=187$ $mM^{-1}\cdot cm^{-1}$ (*18*)] indicates splitting of the Soret peak with a uniform blue shift and smaller intensity. In Gouterman's four-orbital model for the electronic spectra of porphyrins (*21*), the Soret band arises from the electronic transition from the degenerated a_{1u} and a_{2u} orbitals to the lowest vacant e_g orbital. The substitution of the porphyrin ring by meso nitrogens breaks the degeneracy of the two orbitals of porphyrin (*21*), which causes lower intensity of the Soret band, as found in phthalocyanines. The visible spectra of the Mb derivatives in Figs. 1 and 4 exhibit strong similarity to various ferric and ferrous phthalocyanine spectra (*22, 23*). These observations indicate a substantial phthalocyanine character for the diazaheme in Mb.

Binding of Pyridine and Imidazole to Ferrous Mb—One of the characteristic properties of Mb(diazaheme) is the stable coordination of the nitrogenous ligands to the *ferrous* heme. Why does Mb(diazaheme) bind these ligands while native Mb does not? It is very likely that the reactivity of the iron towards the axial ligands is substantially modified in the diazaheme. The axial interactions through the iron and exogenous ligands involve the σ and π bonds. The σ donor strength of the ligands, as estimated from the pK_a (*24*), is pyridine < imidazole < NH_3, whereas the π acceptor order is $NH_3 \ll$ imidazole < pyridine (*23*). The ligand binding constants, *i.e.*, NH_3 (1.7 M^{-1}) < imidazole (200 M^{-1}) < pyridine (11,000 M^{-1}), parallel the π acceptor order of

these ligands. The results suggest the dominant ligand pπ-iron dπ interactions in Mb(diazaheme).

We have previously reported binding of these ligands to ferrous Mb(monoazaheme) (*12*) as well. However, the binding constants are much smaller than those for Mb(diazaheme). Comparison of the ligation profiles among native Mb (*18*), Mb(monoazaheme) (*12*), and Mb(diazaheme) demonstrates that the ligand pπ-iron dπ interactions become more significant with increasing number of the meso-nitrogens. How do the meso nitrogens cause the reactivity changes of the heme iron? The coordination hole of porphyrin becomes smaller in the order porphyrin > monoazaporphyrin > diazaporphyrin, reflecting a smaller atomic radius of nitrogen. The probable explanation is that the iron dπ orbitals are deformed in the narrow cavity to facilitate overlap with the ligand pπ orbitals.

Binding of CN^- and N_3^- to Ferrous Mb—An additional noteworthy finding for ferrous Mb(diazaheme) is the extremely high affinity for CN^- and N_3^-. This is in contrast to the native Mb, which does not bind the anionic ligands in the deoxy state. The iron dπ-ligand pπ interactions seem less important for these ligands because they adopt bent configurations in Mb (*25, 26*). The kinetic analyses reveal quite distinct profiles between anionic ligands and neutral bases. As found in Table II, the ligation of CN^- and N_3^- is facilitated by the much smaller k_{off} whereas the bindings of pyridine and imidazole are dominated by the larger k_{on}. The kinetic dissociation rates of CN^- and N_3^-, which are 10^5 to 10^7-fold smaller than those for pyridine and imidazole, indicate the stabilization of the iron-ligand bond by electrostatic interactions. As we pointed out above, diazaporphyrin is much more acidic than mesoporphyrin. The stabilization of the ferrous Mb(diazaheme)CN and Mb(diazaheme)-N_3 is primarily caused by the increased positive charge of the iron due to the two electronegative meso-nitrogens.

Functional Aspects—The iron dπ-ligand pπ interactions for neutral axial ligands are enhanced in diazaheme, as evidenced by the binding of imidazole and pyridine to the deoxy Mb. The altered iron-ligand interactions dramatically affect the ligation profiles of O_2, CO, and NO. The O_2 and CO affinities for Mb(diazaheme) are considerably larger than those for native Mb (*15*), suggesting stronger iron-ligand interactions through the π bond, because O_2 and CO are moderate and good π acceptors. In the case of the excellent π-accepting ligand NO, it induces transfer of electron density from heme iron, allowing the proximal imidazole, which is *trans* to the NO, to be broken. It is noteworthy that the 5-coordinate MbNO is less stable in diazaheme (Fig. 6) than in monoazaheme (*12*). The observation suggests that the dissociated proximal histidine has a larger affinity to the heme iron. This is in agreement with the result that exogenous imidazole coordinates to ferrous Mb(diazaheme) with a larger affinity (200 M^{-1}) than to ferrous Mb(monoazaheme) [7 M^{-1} (*12*)].

An enhanced iron axial π-donation in Mb(diazaheme) would lead us to expect a higher O_2 affinity to Mb(diazaheme) than to Mb(monoazaheme) (*12*). Contrary to expectation, however, Mb(diazaheme) has a lower O_2 affinity than Mb(monoazaheme). This unexpected result suggests participation of an additional factor to control the O_2 binding of Mb(diazaheme). It should be noted that diazaporphyrin with pK_3 0.5 is a stronger acid than monoazaporphyrin with pK_3 3.0. The lower pK_3 of diazaporphyrin accounts for the unexpected behavior of Mb(diazaheme), because Sono *et al.* (*15*) have reported that the O_2 affinity of Mb decreases with decreasing pK_3 of porphyrin. The same authors also claimed that the lower pK_3 increases the

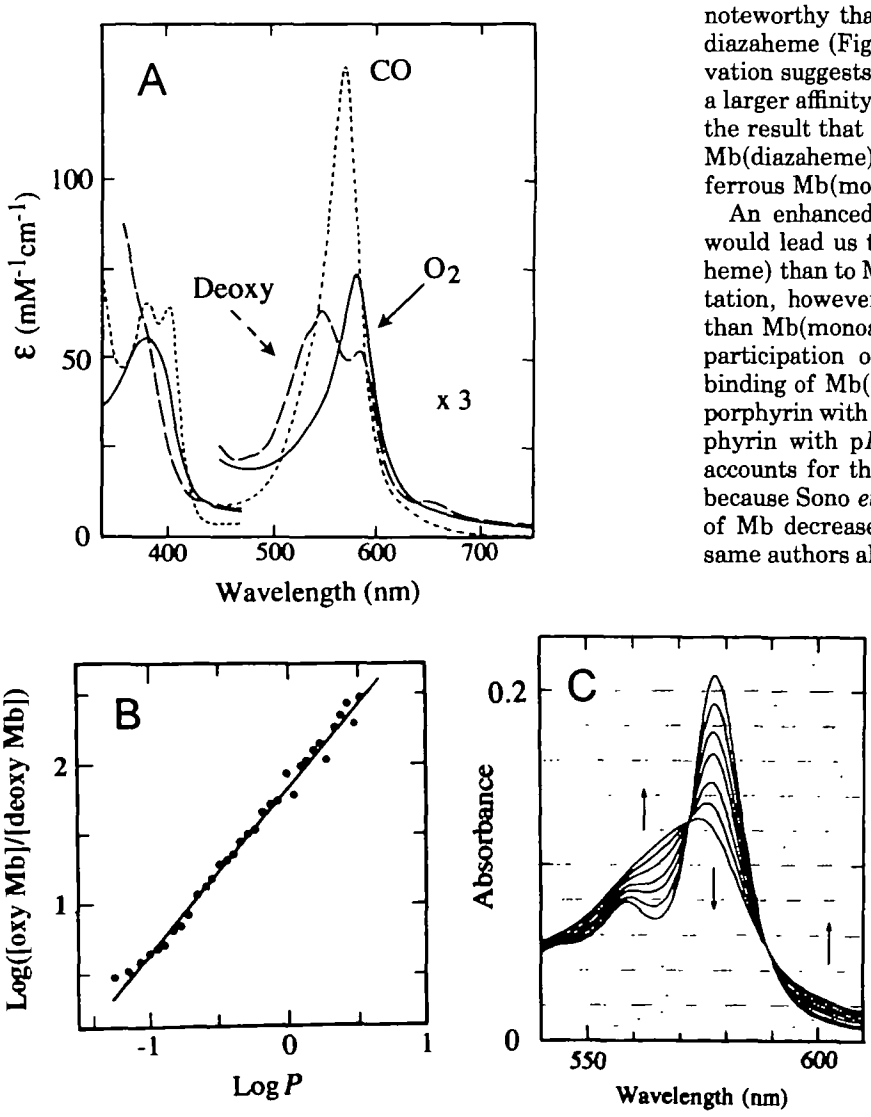

Fig. 5. **Interaction of ferrous Mb(diazaheme) with O_2 and CO.** (A) Visible spectra of the deoxy (----), O_2 (—), and CO (····) derivatives of Mb(diazaheme). All of the spectra were recorded in 0.1 M Tris at pH 7.0 and 20°C. (B) Hill plot of O_2 binding with $n = 1.15$ and $P_{50} = 0.018$ mmHg (3.05×10^7 M^{-1}) as monitored at 580 nm in 0.1 M phosphate at pH 7.0 and 20°C. (C) CO binding to ferrous Mb(diazaheme)pyridine in 0.1 M Tris at pH 7.0, 20°C, and [pyridine] = 0.488 M. The CO concentration was increased from 0 to 1.0, 2.7, 4.4, 7.8, 14.5, and 28.1 μM as indicated by the arrows. The CO affinity monitored at 575 nm is 0.0009 mmHg (8.5×10^8 M^{-1}).

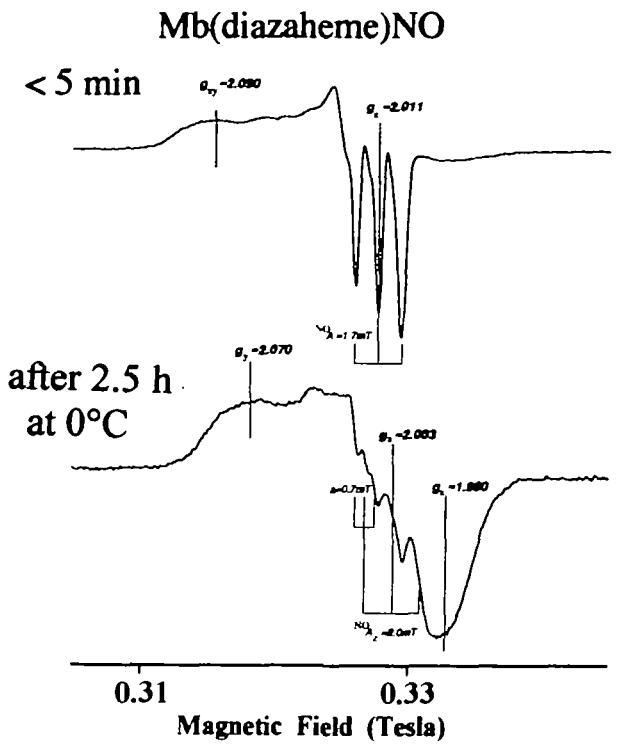

Fig. 6. **Time-dependent EPR of the ^{14}NO derivatives of Mb-(diazaheme) measured at 35 K.** The heme concentration was 2 mM in 0.1 M Tris at pH 7.0.

CO affinity of Mb, in contrast to the case for O_2 (*15*). This is consistent with larger CO affinity of Mb(diazaheme) than Mb(monoazaheme) (*12*). Consequently, the functional anomaly of Mb(diazaheme) primarily arises from an enhanced axial π-bonding of the iron, and is further modulated by the two electron-withdrawing meso-nitrogens.

Relevance to Other Proteins—During the catabolism of aged hemoproteins, the prosthetic group is metabolized to biliverdin by heme oxygenase. Yoshida and Noguchi (*27*) reported that CN^- and N_3^- strongly bind to *ferrous* verdoheme or α-oxyprotoheme (*28*) formed in heme oxygenase. This curious observation has remained to be explained. The binding of CN^- and N_3^- to the ferrous verdoheme-oxygenase complex parallels the results for ferrous Mb(diazaheme) (Fig. 3). An anion binding mechanism common to verdoheme and diazaheme seems to be operating. The electronegative meso-oxygen in verdoheme could place a positive charge on the ferrous iron, like the two meso-nitrogens in diazaheme. An increased positive charge on the ferrous iron allows strong CN^- and N_3^- ligation to the ferrous verdoheme-oxygenase complex.

Finally, it is worth commenting on the implications of Mb(diazaheme) for phthalocyanine-substituted Mb. Water-soluble tetrasulfonated ferrous phthalocyanine is capable of complexing with apoMb to form a reconstituted Mb (*2-4*). The Mb unfortunately binds neither O_2 nor CO because the distal histidine blocks the coordination site (*3, 4*). When phthalocyanines with bulky and charged tetrabenzo groups are introduced into apoMb (*3, 4*), the compact heme pocket can be significantly deformed. Since the imidazole affinity for ferrous Mb increases with increasing number of meso-nitrogens, Mb(phthalocyanine) with tetraazaheme is likely to bind imidazole more tightly than Mb(diazaheme). The possible globin distortion and the high imidazole affinity to the iron could facilitate binding of both the proximal and distal imidazoles to the heme iron, disturbing the O_2 and CO ligation. Thus, the present results can account for the loss of physiological function of the Mb reconstituted with iron phthalocyanines (*2-4*).

REFERENCES

1. Lever, A.B.P., Milaeva, E.R., and Speier, G. (1983) The redox chemistry of metallophthalocyanines in solutions in *Phthalocyanines; Principles and Applications* (Leznoff, C.C. and Lever, A.B.P., eds.) Vol. 3, pp. 3-69, VCH Publications, New York
2. Przywarska-Boniecka, H., Trynda, L., and Antonini, E. (1975) Complexes of metal phthalocyanines with globin as the models of heme proteins. *Eur. J. Biochem.* **52**, 567-573
3. Styness, D.V., Liu, S., and Marcus, H. (1985) Distal histidine coordinates to iron in phthalocyanine-reconstituted myoglobin. *Inorg. Chem.* **24**, 4335-4338
4. Tyagi, L. (1988) Ligand binding and autoxidation of a tetra sulphonated phthalocyanine iron(II)-apomyoglobin complex. *Inorg. Chim. Acta* **151**, 29-31
5. Jackson, A.H. (1978) Azaporphyrins in *The Porphyrins* (Dolphin, D., ed.) Vol. 1, pp. 365-388, Academic Press, New York
6. Fischer, H. and Stern, A. (1940) *Die Chemie des Pyrrols, Band II, Hälfte 2*, pp. 411-414, Akademische Verlagsgesellschaft, Leipzig
7. Harris, R.L.N., Johnson, A.W., and Kay, I.T. (1966) A stepwise synthesis of unsymmetrical porphyrins. *J. Chem. Soc. (C)*, 22-29
8. Fischer, H. and Orth, H. (1937) *Die Chemie des Pyrrols, Band II, Hälfte 1*, p. 91, Akademische Verlagsgesellschaft, Leipzig
9. Fischer, H. and Andersag, H. (1927) Syntheses des β-isokoproporphyrins und der opsopyrrolcarbonsäure. *Justus Liebigs Ann. Chem.* **458**, 117-148
10. Adler, A.D., Longo, F., Kampas, F., and Kim, J. (1970) On the preparation of metalloporphyrins. *J. Inorg. Nucl. Chem.* **32**, 2443-2445
11. Fuhrhop, J.-H. and Smith, K.M. (1975) *Porphyrins and Metalloporphyrins* (Smith, K.M., ed.) pp. 757-869, Elsevier, Amsterdam
12. Neya, S., Kaku, T., Funasaki, N., Shiro, Y., Iizuka, T., Imai, K., and Hori, H. (1995) Novel ligand binding properties of the myoglobin reconstituted with monoazahemin. *J. Biol. Chem.* **270**, 13118-13123
13. Imai, K. (1981) Measurements of accurate oxygen equilibrium curves by an automatic oxygenation apparatus in *Methods in Enzymology* (Antonini, E., Rossi-Bernardi, L., and Chiancone, E., eds.) Vol. 76, pp. 438-449, Academic Press, New York
14. Hayashi, A., Suzuki, T., and Shin, M. (1973) An enzymic reduction system for metmyoglobin and methemoglobin, and its application to functional studies of oxygen carriers. *Biochim. Biophys. Acta* **310**, 309-316
15. Sono, M., Smith, P.D., McCary, J.A., and Asakura, T. (1976) Kinetic and equilibrium studies of the reactions of heme-substituted horse heart myoglobin with oxygen and carbon monoxide. *J. Biol. Chem.* **251**, 1418-1426
16. Grigg, R., Hamilton, R.J., Jozefowicz, M.L., Rochester, C.H., Rerrell, R.J., and Wickwar, H. (1973) A spectroscopic study of the protonation of porphyrins and corroles. *J. Chem. Soc. Perkin Trans.* **2**, 407-417
17. Hambright, P. (1975) Dynamic coordination chemistry of metalloporphyrins in *Porphyrins and Metalloporphyrins* (Smith, K.M., ed.) pp. 233-278, Elsevier, Amsterdam
18. Antonini, E. and Brunori, M. (1971) *Hemoglobin and Myoglobin in Their Reactions with Ligands*, pp. 19 and 229-233, North Holland, Amsterdam
19. Hori, H. (1971) Analysis of the principal *g*-tensors in single crystals of ferrimyoglobin complexes. *Biochim. Biophys. Acta* **251**, 227-235
20. Neya, S. and Funasaki, N. (1988) Proton NMR study of the myoglobin reconstituted with *meso*-tetra(*n*-propyl)hemin. *Bio-*

chim. Biophys. Acta **952**, 150-157
21. Gouterman, M. (1978) Optical spectra and electronic structure of porphyrins and related rings in *The Porphyrins* (Dolphin, D., ed.) Vol. 3, pp. 1-165, Academic Press, New York
22. Kennedy, B.J., Murray, K.S., Zwack, P.R., Homborg, H., and Kalz, W. (1986) Spin state in iron(III) phthalocyanines studies by Mössbauer, magnetic susceptibility, and EPR measurements. *Inorg. Chem.* **25**, 2539-2545
23. Ough, E.A. and Stillman, M.J. (1994) Analysis of the absorption and magnetic circular dichroism spectra of iron(II) phthalocyanine. *Inorg. Chem.* **33**, 573-583
24. Weast, R.C., ed. (1978-1979) *CRC Handbook of Chemistry and Physics*, D-200-201, 59th ed., CRC Press, FL
25. Neya, S., Funasaki, N., Sato, T., Igarashi, N., and Tanaka, N. (1993) Structural analysis of the myoglobin reconstituted with iron porphine. *J. Biol. Chem.* **268**, 8935-8942
26. Stryer, L., Kendrew, J.C., and Watson, H.C. (1964) The mode of attachment of the azide ion to sperm whale metmyoglobin. *J. Mol. Biol.* **8**, 96-104
27. Yoshida, T. and Noguchi, M. (1984) Features of intermediary steps around the 688-nm substance in the heme oxygenase reaction. *J. Biochem.* **96**, 563-570
28. Yoshida, T. (1987) Heme degradation by heme oxygenase system. *Protein, Nucleic Acid, and Enzyme* **32**, 822-829